Theor Chem Acc (2012) 131:1068
DOI 10.1007/s00214-011-1068-8

REGULAR ARTICLE

# A full-dimensional time-dependent wave packet study of the OH + CO → H + $CO_2$ reaction

**Shu Liu · Xin Xu · Dong H. Zhang**

Received: 1 July 2011 / Accepted: 3 August 2011 / Published online: 11 January 2012


**Abstract** Full-dimensional time-dependent wave packet calculations were made to study the $OH + CO \rightarrow H + CO_2$ reaction on the Lakin–Troya–Schatz–Harding potential energy surface. Because of the presence of deep wells supporting long-lived collision complex, one needs to propagate the wave packet up to 450,000 a.u. of time to fully converge the total reaction probabilities. Our calculation revealed that the CO bond was substantially excited vibrationally in the complex wells, making it necessary to include sufficient CO vibration basis functions to yield quantitatively accurate results for the reaction. We calculated the total reaction probabilities from the ground initial state and two vibrationally excited states for the total angular momentum $J = 0$. The total reaction probability for the ground initial state is quite small in magnitude with many narrow and overlapping resonances due to the small complex-formation reaction probability and small probability for complex decaying into product channel. Initial OH vibrational excitation considerably enhances the reactivity because it enhances the probability for complex decaying into product channel, while initial CO excitation has little effects on the reactivity. We also calculated the reaction probabilities for a number of $J > 0$ states by using the centrifugal sudden approximation. By doing some calculations with multiple *K*-blocks included, we found that the centrifugal sudden approximation can be employed to calculate the rate constant for the reaction rather accurately. The calculated rate constants only agree with experimental measurements qualitatively, suggesting more theoretical studies be carried out for this prototypical complex-formation four-atom reaction.

**Keywords** Complex-forming reactions · Quantum scattering · Reaction resonance · Time-dependent wave packet method

## 1 Introduction

Because of its crucial role in the conversion of CO to $CO_2$, the $OH + CO \rightarrow H + CO_2$ reaction is important to both atmospheric [1] and combustion chemistry [2]. Due to the presence of two deep wells along the reaction path which support long-lived collision complex HOCO in both *trans* and *cis* configurations, the reaction dominated by pronounced resonances has become a prototype recently for complex-forming four-atom reactions, just as $H_2 + OH \rightarrow H + H_2O$ is for direct four-atom reactions.

The OH + CO reaction has been the subject of many experimental studies [3–12]. The measured thermal rate constants show a strong non-Arrhenius dependence on temperature [13–15]. They are nearly independent on temperature between 80 and 500 K. On the contrary, at temperatures higher than 500 K, they sharply increase with temperature. This behavior has been attributed to the presence of an intermediate HOCO complex with non-zero barriers in the entrance (OH + CO) and exit (H + $CO_2$) channels. The molecular beam experiment carried out by Alagia et al. [16] showed strong peaks in both the forward

Published as part of the special collection of articles celebrating the 50th anniversary of Theoretical Chemistry Accounts/Theoretica Chimica Acta.

S. Liu · X. Xu · D. H. Zhang (✉)
State Key Laboratory of Molecular Reaction Dynamics and Center for Theoretical and Computational Chemistry, Dalian Institute of Chemical Physics, Chinese Academy of Sciences, Dalian 116023, People's Republic of China
e-mail: zhangdh@dicp.ac.cn

and backward directions, indicating the existence of intermediate species. Another unusual aspect of the OH + CO reactant system is that it can form two hydrogen-bonded, van der Waals complexes, OH–CO and OH–OC, prior to the entrance channel transition state. Lester and co-workers have experimentally measured the existence of the linear OH–CO complex using infrared action spectroscopy [17]. Complementary electronic structure calculations show that there is a reaction pathway connecting the OH–CO complex to the HO–CO transition state.

Extensive theoretical studies have been carried out for this reaction and its reverse. In 1987, the first global analytic potential energy surface (PES) was constructed by Schatz, Fitzcharles, and Harding (denoted as SFH) based on the many-body expansion approach [18]. Following that, a few more PESs, such as KSW [19] PES, BS [20] PES, and YMS [21] PES, were constructed to study the reaction more accurately. In 2003, Lakin, Troya, Schatz, and Harding modified the existing many-body expansion PES further based on their new ab initio calculations to give a more accurate description of the reactant channel complexes [22]. Schatz and co-workers performed substantial quasi-classical trajectory (QCT) calculations on the new PES, known as the LTSH PES, to assess the influence of the surface changes on the reaction dynamics. It was found that the presence of the reactant channel wells enhanced the reactivity at intermediate range of energies. While the thermal rate constants obtained from the QCT calculation were smaller than experiment results, likely due to an excessively high and/or broad exit channel barrier on the surface [22, 23].

The OH + CO reaction presents a huge challenge to quantum dynamics. The combination of a relatively long-lived collision complex and three heavy atoms in this reaction makes the rigorous quantum scattering calculations difficult. In 1995, Zhang and Zhang [24] carried out a potential-averaged five-dimensional (PA5D) quantum dynamical study on SFH PES. A few years later, Kroes and co-workers obtained the PA5D total reaction probabilities for total angular momentum $J = 0$ on YMS and LTSH PES and performed 6D calculations on BS PES [25]. Medvedev et al. carried out a six-dimensional quantum wave packet study on LTSH PES, but only with 2 vibrational basis functions used for non-reactive CO bond.

In the present work, we used the time-dependent wave packet (TDWP) method to study the title reaction on LTSH PES in full dimensions. We calculated the initial-state selected total reaction probabilities from the ground state as well as some vibrational excited states for the total angular momentum $J = 0$. The total reaction probabilities for the ground initial state for $J > 0$ were also computed under the centrifugal sudden (CS) approximation. To assess the accuracy of the CS approximation, we also calculated the total reaction probabilities for a few $J > 0$ initial states with multiple $K$ components included. The rest of this paper is organized as follows. In Sect. 2, we present the theory of the full-dimensional TDWP treatment to diatom–diatom reactions and some computational details. Section 3 contains our results, including total reaction probabilities, studies of reagent vibrational excitation, and the accuracy of the CS approximation for this reaction. In Sect. 4, we summarize our conclusions.

## 2 Theory

We outline the theory of the TDWP method for calculating the initial state selected total reaction probability for a diatom–diatom reaction AB + CD → A + BCD in full dimensions. For details, please refer Refs. [26, 27]. The Hamiltonian expressed in the reactant Jacobi coordinates shown in Fig. 1 for a given total angular momentum $J$ can be written as

$$\hat{H} = -\frac{\hbar^2}{2\mu}\frac{\partial^2}{\partial R^2} + h_1(r_1) + h_2(r_2) + \frac{\mathbf{j_1}}{2\mu_1 r_1^2} + \frac{\mathbf{j_2}}{2\mu_2 r_2^2} + \frac{(\mathbf{J} - \mathbf{j_{12}})^2}{2\mu R^2} + V(r_1, r_2, R, \theta_1, \theta_2, \varphi) \quad (1)$$

where $\mu$ is the reduced mass between the center of mass of OH and CO, $\mathbf{J}$ is the total angular momentum operator, and $\mathbf{j}_1$ and $\mathbf{j}_2$ are the rotational angular momentum operators of OH and CO, which are coupled to form $\mathbf{j}_{12}$. The diatomic reference Hamiltonian $h_i(r_i)$ is defined as

$$h_i(r_i) = -\frac{\hbar^2}{2\mu_i}\frac{\partial^2}{\partial r_i^2} + V_i(r_i). \quad (2)$$

The time-dependent wave function can be expanded in terms of the translational basis of $R$, the vibrational basis $\phi_{v_i}(r_i)$, and the BF rovibrational eigenfunction as

$$\Psi^{JM\epsilon}_{v_0 j_0 K_0}(\mathbf{R}, \mathbf{r_1}, \mathbf{r_2}, t) = \sum_{n,v,j,K} F^{JM\epsilon}_{nvjK,v_0 j_0 K_0}(t) u_n^{v_1}(R)\phi_{v_1}(r_1)\phi_{v_2}(r_2) Y^{JM\epsilon}_{jK}(\hat{R}, \hat{r}_1, \hat{r}_2). \quad (3)$$

The BF total angular momentum eigenfunction can be written as

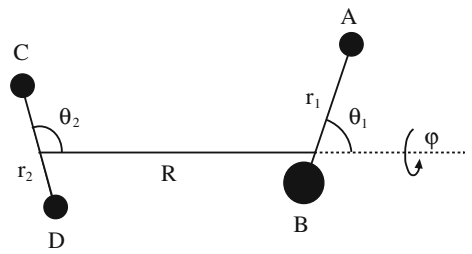


**Fig. 1** Jacobi coordinates for the reaction AB + CD → A + BCD. The angle $\varphi$ is the out-of-plane torsional angle

$$Y_{jK}^{JM\epsilon} = (1+\delta_{K0})^{-1/2}\sqrt{\frac{2J+1}{8\pi}} \times \left[D_{K,M}^{J} Y_{j_1 j_2}^{j_{12}K} + \epsilon(-1)^{j_1+j_2+j_{12}+J} D_{-K,M}^{J} Y_{j_1 j_2}^{j_{12}-K}\right], \quad (4)$$

where $D_{K,M}^{J}$ is the Wigner rotation matrix [28], $\epsilon$ is the total parity of the system and $K$ is the projection of total angular momentum on the BF axis, and $Y_{j_1 j_2}^{j_{12}K}$ is the angular momentum eigenfunction of $j_{12}$,

$$Y_{j_1 j_2}^{j_{12}K} = \sum_{m_1} \langle j_1 m_1 j_2 K - m_1 | j_{12} K\rangle \times y_{j_1 m_1}(\theta_1, 0) y_{j_2 K-m_1}(\theta_2, \phi) \quad (5)$$

where $y_{jm}$ are spherical harmonics. From Eq. 4, one can see that the $K = 0$ block can only appear when $\epsilon(-1)^{j_1+j_2+j_{12}+J} = 1$.

We construct an initial wave packet $\psi_i(0)$ and propagate it using the split-operator method. The total reaction probability for that specific initial state $i$ for a whole range of energies can be obtained by evaluating the reactive flux at a dividing surface $s = s_0$

$$P_i^R(E) = \frac{\hbar}{m_s}\mathrm{Im}[\langle \psi_{iE}^{+}|\delta(s-s_0)\frac{\partial}{\partial s}|\psi_{iE}^{+}\rangle]. \quad (6)$$

$\psi_{iE}^{+}$ denotes the time-independent (TI) wavefunction, which can be obtained by performing a Fourier transform of the time-dependent wave function as

$$\langle \psi_{iE}^{+}\rangle = \frac{1}{a_i(E)}\int_{-\infty}^{\infty} e^{\frac{i}{\hbar}(E-H)t}|\psi_i(0)> \mathrm{d}t. \quad (7)$$

The coefficient $a_i(E)$ is the overlap between the initial wave packet and the energy-normalized asymptotic scattering function, $a_i(E) = \langle \phi_{iE}|\psi_i(0)\rangle$.

The numerical parameters for the wave packet propagation were as follows: a total of 228 sine functions (among them 36 for the interaction region) were employed for the translational coordinate $R$ in a range of [3.0, 16.0] $a_0$. Five OH vibrational basis functions were used in the asymptotic region, while 32 were used in the interaction region to expand the wave function for $r_1$ going from 1.0 $a_0$ to 5.5 $a_0$. For rotational degrees of freedom, we used 36 OH rotational states and 91 CO rotational states. A total number of 7 vibrational basis functions were used for non-reactive CO bond to get converged reaction probabilities for collision energy up to 0.4 eV. The initial Gaussian wave packet was centered at 12.5 $a_0$. A dividing surface at 3.2 $a_0$ was used for flux analysis. The wave packet propagation was carried out using a time increment of 10 a.u. A typical calculation for the total angular momentum $J = 0$ takes about 300 h on 8 workstations each with 8 CPU cores.

## 3 Results

Figure 2 shows the convergence of total reaction probabilities for the ground initial state with respect to the propagation time for $J = 0$. At short propagation time, the probabilities are small and the resonance structures are not significant. As propagation time extends, the overall magnitude gradually increases and the resonance structures become more pronounced. The probabilities are well converged after the wave packet is propagated for around 450,000 a.u. As can be seen, the converged total reaction probability shows many narrow but overlapping resonances in the low collision energy region, apparently due to the long-lived HOCO complex. It gradually becomes relatively smooth for collision energy above 0.3 eV.

To give some clues on the role of CO vibration in the reaction, we depict in Fig. 3a the vibrational potentials for CO in asymptotic region and in the wells. It can be seen that the CO equilibrium distance in the wells is longer than that for the free CO by about 0.06 $a_0$. As a result, the CO bond initially in the ground state has some population on the excited states once moving into the wells as shown in Fig. 3b. As the time propagation goes on, the CO bond for the complex gets more excited as monitored from the average bond energy shown in Fig. 3c. At $T \sim 35,000$ a.u., it more or less reaches a steady state with a population shown in Fig. 3b. Thus, it is clear that the CO bond is highly excited in the complex, and it absorbs about 0.35 eV of energy resulting from the complex formation.

The substantial excitation of CO bond in the complex wells indicates that the non-reactive CO bond does not act as a spectator, as it is described by the PA5D model, in the reaction. Kroes and co-workers have obtained the PA5D

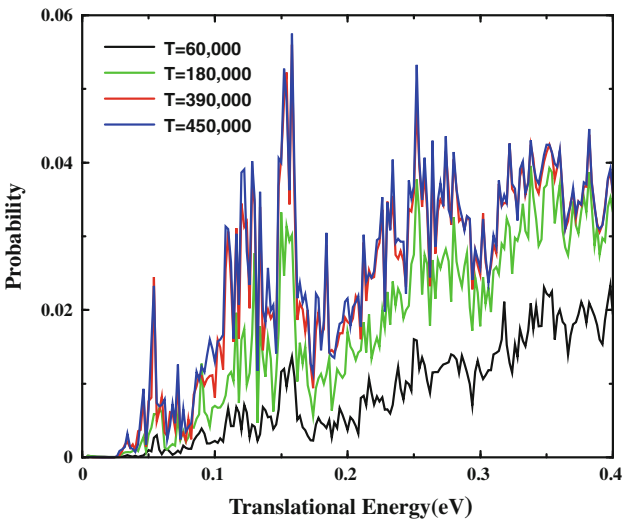


**Fig. 2** Total reaction probabilities for the ground initial state of the OH + CO reaction on the LTSH PES at wave packet propagation time of $T$ = 60,000, 180,000, 390,000, and 450,000 a.u.

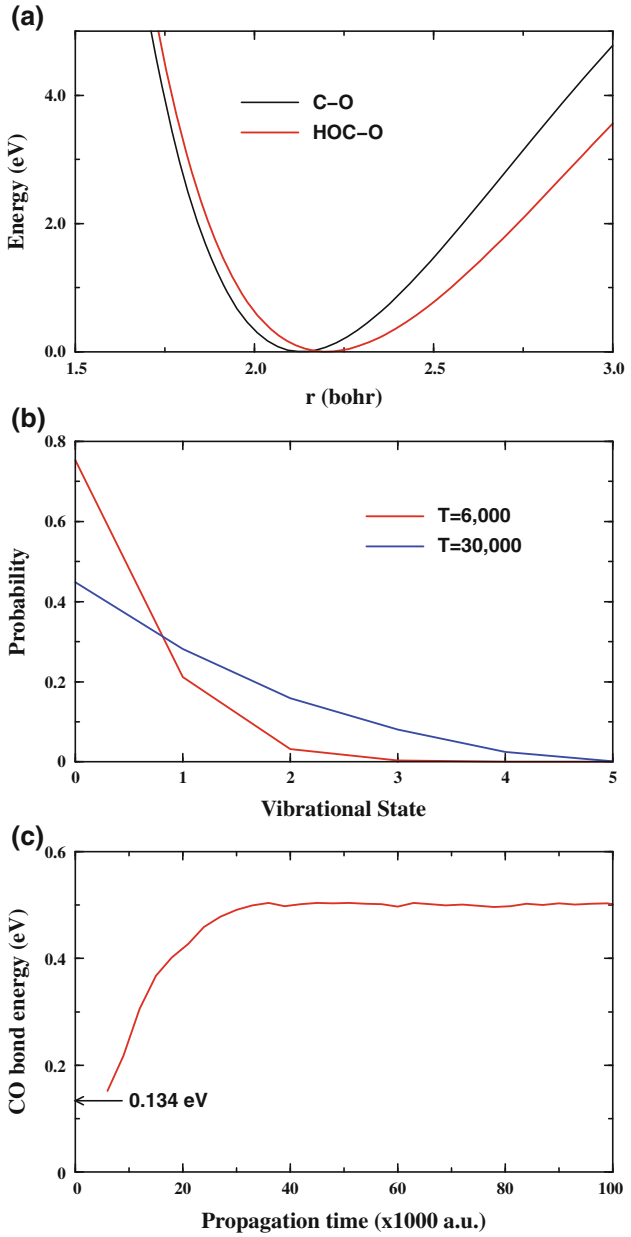


**Fig. 3** **a** Vibrational potentials for CO in asymptotic region and in the wells; **b** population probability of CO in the wells at propagation time of 6,000 and 30,000 a.u.; **c** average bond energy of the CO bond in the wells as a function of time. We start to calculate it from $T$ = 6,000 when a non-negligible portion of wave packet has moved in the wells. The *horizontal arrow* indicates the ground state energy of free CO

reaction probability on LTSH PES [25], which is quite different from our full-dimensional reaction probability in detail. So the PA5D treatment is incapable of yielding quantitative results for the title reaction, although it works very well for the $H_2 + OH$ reaction.

Although the $OH + CO \rightarrow H + CO_2$ reaction on the LTSH PES is exothermic by about 0.967 eV and has only a low barrier in the entrance channel along the minimum energy path, the reaction probability is generally small. It turned out that the majority of wave packet was reflected back to the entrance valley at $R = 4.6\ a_0$ prior to entering the HOCO well, in accord with the molecular beam experimental results of Liu and coworkers [8]. Figure 4a shows the complex-formation probability, $P_c$, as a function of collision energy obtained by calculating the flux into the wells [29]. As seen, the complex-formation probability rises quickly at the threshold energy of 0.02 eV, reaches 8% at Ec = 0.05 eV, and then increases slowly with further increase in collision energy to 21% at Ec = 0.4 eV, indicating that the entrance cone into the HOCO complex well is rather small. The ratio between the reaction probability and complex-formation probability shown in Fig. 4c gives the probability for the complex decaying into product channel, $P_d$. In low collision energy region, $P_d$ fluctuates substantially from a few percent to up to 50% around Ec = 0.15 eV. For higher collision energies, it oscillates about 20%. This states that the complex decays primarily back to reactant channel, because the barrier separating complexes from products is higher and broader than the barrier separating complexes from reactants.

The small entrance cone to the complex well and relatively high and broad barrier separating complexes from products on the LTSH PES not only make the reaction probability small, but also make the decay of complex very slow. Consequently, to converge the reaction probability, one needs to propagate the wave packet for a very long time, much longer than that for the SFH PES of about 90,000 a.u. [24].

Figure 4a and b also show the total reaction probabilities and complex-formation probabilities for the OH or CO vibrationally excited initial states as a function of translational energy. As expected, the complex-formation probabilities are very close to each other for these three initial states, in particular in low collision energy region, while the reaction probabilities behave rather differently. Although the OH vibrational excitation essentially does not reduce the threshold energy for the reaction because the reaction threshold is determined by the entrance barrier as found for the complex-formation probabilities, it enhances the reactivity considerably. The reaction probability for that initial state rises quickly in the collision energy range from threshold to about 0.06 eV. It then increases slower with the further increase in the collision energy, essentially with the same slope as that for the ground initial state. At the collision energy of 0.4 eV, the probability for the OH ($v = 1$) initial state is larger than that for the ground state by a factor of 1.8. It also can be seen that the OH ($v = 1$) reaction probability is much less oscillatory compared to the ground initial state in the low collision energy region. Consequently, it converges at a propagation time of 270,000 a.u., much shorter than that for the ground initial

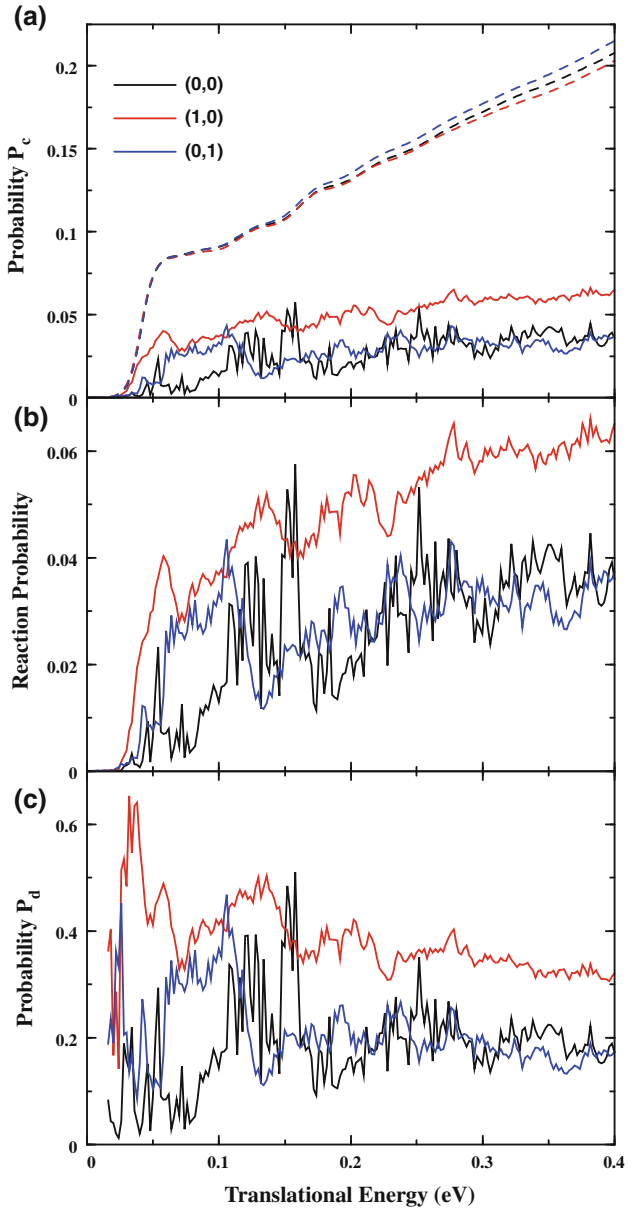


**Fig. 4** **a** Complex-formation probabilities (in *dashed lines*), $P_c$, and corresponding total reaction probabilities (in *solid lines*) for the ground and two vibrationally excited states as a function of collision energy on the LTSH PES; **b** total reaction probabilities as shown in **a** except in a smaller *y*-axis range; **c** probability for the complex decaying into product channel, $P_d$, as a function of collision energy

state of 450,000 a.u. On the other hand, no substantial enhancement on the reaction probability is observed for the vibrational excitation of CO to the first excited state as shown in Fig. 4b, except in a small energy range around 0.1 eV. We also note that Kroes and co-workers also calculated the 6D QCT reaction probabilities for CO ($v = 1$) on the LTSH PES [30], which are in reasonable agreement with our QM result.

Since the complex-formation probabilities, $P_c$, for these three initial states are essentially the same as shown in Fig. 4a, different reaction probabilities mean that the probabilities for the complex decaying into product channel, $P_d$, for the three states are different. As shown in Fig. 4c, in almost entire energy region, $P_d$ for OH ($v = 1$) is considerably larger than the other two states. In high-energy region $P_d$ for CO ($v = 1$) is very close to that for the ground initial state. In low-energy region, each of them has an energy window with substantially larger $P_d$, and somehow the energy window for CO ($v = 1$) is lower in energy by about 0.045 eV than that for the ground initial state. Therefore, it is clear that increase in complex energy on the coordinates other than on the OH coordinate does not increase the probability for complex decaying into product channel except near energy threshold, while increase in energy on OH bond in complex does increase the probability, and the excitation energy initially deposited on OH bond remains to some extent on the bond in the complex.

The total reaction probabilities from the ground initial state for a number of total angular momentum $J$ were calculated under the CS approximation. Figure 5 presents the results for $J = 30$ and 50. As seen, the $J > 0$ CS reaction probability curves resemble the $J = 0$ curve very well, except for a threshold energy shift caused by the centrifugal potential and a small decrease in overall magnitude with the increase of $J$.

To check the accuracy of the CS approximation for the reaction with only $K = 0$ block included, we made some $J > 0$ calculations with more than one $K$-block. This kind of calculations for $J > 0$ is extremely time-consuming as the computational effort increases by a factor of $2 \times NK + 1$ (where $NK$ is the number of $K$-blocks) compared with the CS calculation. Figure 6 shows the $J = 20$ total reaction probabilities calculated with $NK = 1$ (CS),

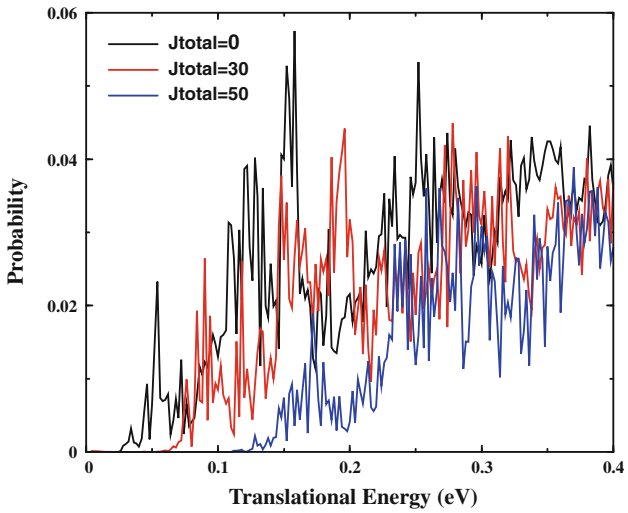


**Fig. 5** Total reaction probabilities for $J = 30$ and 50 with CS approximation for the OH + CO reaction as a function of collision energy

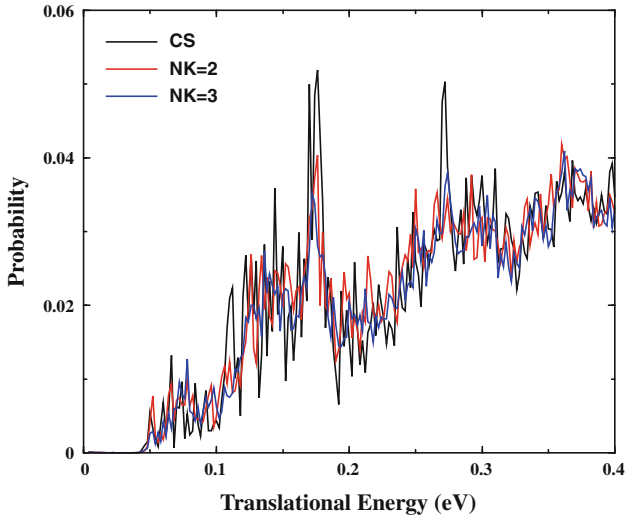


**Fig. 6** Comparison of the CS reaction probability for $J = 20$ with the $NK = 2$, 3 results

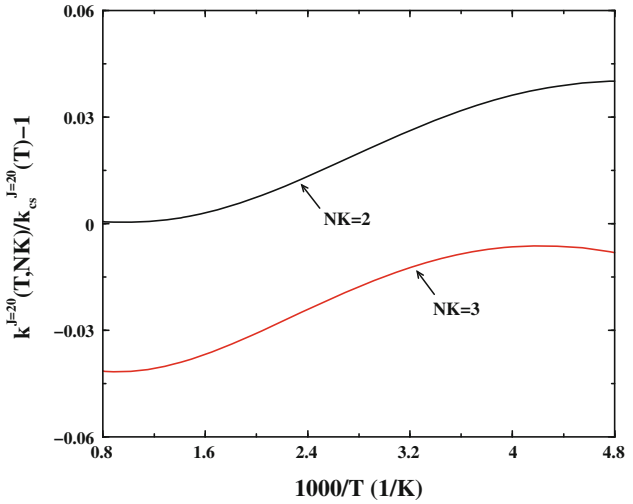


**Fig. 7** Differences between CS and $NK = 2$, 3 rate constants for partial wave $J = 20$

$NK = 2$, and $NK = 3$. Overall, the CS probability agrees with the $NK > 1$ results rather well, but the probability curve becomes increasingly smoother as $NK$ increases. Although the difference between the $NK = 2$ and 3 probabilities is rather small, it seems that 3 $K$-blocks are not sufficient to yield a full convergence on the total reaction probability even for $J = 20$.

However, if one is only interested in the rate constant, the CS approximation actually can be employed without any significant deterioration in accuracy for this reaction. In Fig. 7, we show the difference between CS and $NK = 2$, 3 rate constants for $J = 20$ measured in term of $k^{J=20}(T, NK)/k_{cs}^{J=20}(T) - 1$, where $k^J(T, NK)$ is rate constant for partial wave $J$ given by

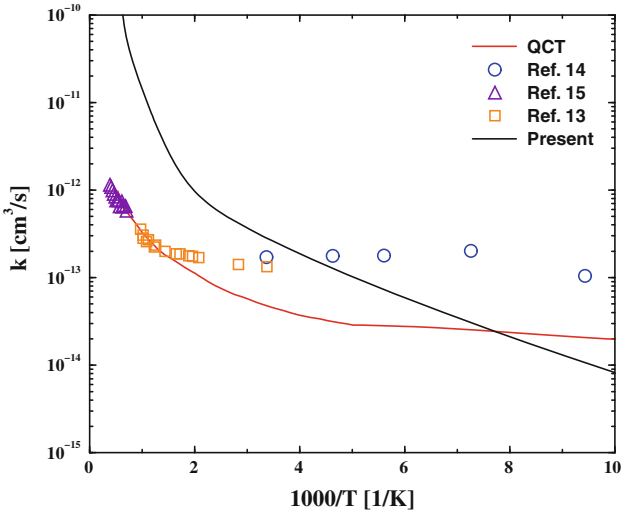


**Fig. 8** CS rate constant for the ground initial state for the title reaction compared with the previous QCT result on the same PES and experimental data of Frost et al. ([14], *circles*), Golden et al. ([15], *triangles*), and Ravishankara and Thompson ([13], *squares*)

$$k^J(T, NK) = \int_0^\infty \mathrm{d}E \mathrm{e}^{-E/k_bT} P^J(E, NK). \quad (8)$$

In the entire temperature region shown, $k^{J=20}(T, NK = 2)$ is only a few percents larger than $k_{cs}^{J=20}(T)$, and $k^{J=20}(T, NK = 3)$ is only by a few percents smaller than $k_{cs}^{J=20}(T)$, despite the fact that the details of the corresponding reaction probabilities differ considerably as shown in Fig. 6. Our test calculation also showed that the difference between the CS rate constant for $J = 50$ and the corresponding $NK = 3$ rate constant is <10% in the valid temperature region. Therefore in the temperature region of Fig. 7, where the thermal rate constant is dominated by contributions from partial waves with $J$ up to 50, the CS approximation can be used to calculate the thermal rate constant for this reaction with a reasonable accuracy.

With long wave packet propagation time in this reaction, it is a formidable task at present to calculate the total reaction probabilities for many partial waves to obtain integral cross sections for the reaction. Instead, we calculated the rate constant for the ground initial state by using the J-shifting scheme [31]. Figure 8 shows the CS rate constant in a temperature range from 100 to 1,700 K, in comparison with the QCT result on the same PES [23] and some experimental results [13–15]. At $T = 100$ K, the QM rate is smaller than both QCT and experimental results. However, as temperature increases, the QM rate increases much faster than QCT and experimental results, which becomes the largest at $T \sim 250$ K. One should note that our calculation is for initial ground rovibrational state, while the experimental measurements are for the thermal

averaging over initial rotations of the reagents. Thus, the discrepancy between the experiment and present calculation may come from the defects of the PES, or the neglect of influence of reagent rotational excitations, or both. More theoretical studies should be carried out to shed light on the discrepancy, to eventually lead a quantitative agreement between theory and experiment on this prototypical complex-formation four-atom reaction.

## 4 Conclusions

We carried out extensive TDWP calculations on the $OH + CO \rightarrow H + CO_2$ reaction on the LTSH PES. Because of the presence of deep wells supporting long-lived collision complex HOCO, one needs to propagate wave packets up to 450,000 a.u. of time to fully converge the pronounced resonance structures in the total reaction probabilities. We calculated the total reaction probabilities for the ground initial state as well as two vibrational excited states for total angular momentum $J = 0$. The total reaction probability for the ground initial state is quite small in magnitude with many narrow and overlapping resonances, because (1) the complex-formation reaction probability is quite small due to the small entrance cone into the HOCO complex wells; (2) the reactive complex decays primarily back to reactant channel as the barrier separating complexes from products is higher and broader than the barrier separating complexes from reactants. Our calculation also revealed that the CO bond was substantially excited vibrationally in the complex wells, making the PA5D method incapable of yielding quantitative results for the reaction.

We also investigated the effects of initial vibrational excitation on the reaction. It is found that initial vibrational excitation of OH considerably enhances the reactivity of the system, while initial vibrational excitation of CO has no significant enhancement to reaction probability. Because the complex-formation probabilities for these three initial states are found to be very close to each other, reactivity enhancement with the OH excitation is clearly due to the fact that initial OH excitation enhances the probability for the complex decaying into product channel.

The total reaction probabilities were calculated for a number of $J > 0$ states by using the CS approximation. To assess the validity of the CS approximation for the reaction, we also calculated some $J > 0$ reaction probabilities for the ground initial state with multiple $K$-blocks included. Overall, the agreement between the CS and $NK = 2$, 3 calculations is reasonably good, but the reaction probabilities become increasingly smoother as the number of $K$-blocks increases. While one is only interested in the thermal rate constant, the CS approximation can be employed without any significant deterioration in accuracy for this reaction. We found that the calculated CS rate constants only agree with experimental measurements qualitatively, suggesting more theoretical studies be carried out for this prototypical complex-formation four-atom reaction.

**Acknowledgments** This work was supported by the National Natural Science Foundation of China (Grant Nos. 20833007 and 90921014), the Chinese Academy of Sciences, and Ministry of Science and Technology of China.

## References

1. Finlayson-Pitts BJ, Pitts JN (2000) Chemistry of the upper and lower atmosphere. Academic press, San Diego
2. Miller JA, Kee RJ, Westbrook CK (1990) Annu Rev Phys Chem 41:345
3. Smith IWM, Zellner R (1973) J Chem Soc Faraday Trans 2(69):1617
4. Jonah CD, Mulac WA, Zeglinski P (1984) J Phys Chem (US) 88
5. Gardiner WC Jr (1977) Acc Chem Res 10:326
6. Brunning J, Derbyshire DW, Smith IWM, Williams MD (1988) J Chem Soc Faraday Trans 2 84:105
7. Fulle D, Hamann HF, Hippler H, Troe J (1996) J Chem Phys 105:983
8. Sonnenfroh DM, Macdonald RG, Liu K (1991) J Chem Phys 94:6508
9. van Beek MC, Ter Meulen JJ (2001) J Chem Phys 115:1843
10. Scherer NF, Khundkar LR, Bernstein RB, Zewail AH (1987) J Chem Phys 87:1451
11. Rice JK, Baronavski AP (1991) J Chem Phys 94:1006
12. Ionov SI, Brucker GA, Jaques C, Valachovic L, Wittig C (1993) J Chem Phys 99:6553
13. Ravishankara AR, Thompson RL (1983) Chem Phys Lett 99:377
14. Frost MJ, Sharkey P, Smith IWM (1991) Faraday Discuss Chem Soc 91:305
15. Golden DM, Smith GP, McEwen AB, Yu CL, Eiteneer B, Frenklach M, Vaghjiani GL, Ravishankara AR, Tully FP (1998) J Phys Chem A 102:8598
16. Alagia M, Balucani N, Casavecchia P, Stranges D, Volpi GG (1993) J Chem Phys 98:8341
17. Lester MI, Pond BV, Anderson DT, Harding LB, Wagner AF (2000) J Chem Phys 113:9889
18. Schatz GC, Fitzcharles MS, Harding LB (1987) Faraday Discuss Chem Soc 84:359
19. Kudla K, Schatz GC, Wagner AF (1991) J Chem Phys 95:1635
20. Bradley KS, Schatz GC (1997) J Chem Phys 106:8464
21. Yu HG, Muckerman JT, Sears TJ (2001) Chem Phys Lett 349:547
22. Lakin MJ, Troya D, Schatz GC, Harding LB (2003) J Chem Phys 119:5848
23. Medvedev DM, Gray SK, Goldfield EM, Lakin MJ, Troya D, Schatz GC (2004) J Chem Phys 120:1231
24. Zhang DH, Zhang JZH (1995) J Chem Phys 103:6512
25. Valero R, McCormack DA, Kroes GJ (2004) J Chem Phys 120:4263
26. Zhang DH, Zhang JZH (1994) J Chem Phys 101:1146
27. Zhang DH, Lee SY (1999) J Chem Phys 110:4435
28. Rose M (1957) Elementary theory of angular momentum. Wiley, New York
29. Lin S, Guo H (2004) J Chem Phys 120:9907
30. Valero R, Kroes GJ (2004) Phys Rev A 70:040701
31. Zhang DH, Zhang JZH (1999) J Chem Phys 110:7622